ACS Catalysis

Research Article

pubs.acs.org/acscatalysis

Selectivity in Ring-Opening Metathesis Polymerization of *Z*-Cyclooctenes Catalyzed by a Second-generation Grubbs Catalyst

Henry Martinez, Pere Miró, Patrick Charbonneau, Marc A. Hillmyer,* and Christopher J. Cramer*

Department of Chemistry, Chemical Theory Center, and Supercomputing Institute, University of Minnesota, 207 Pleasant St. SE, Minneapolis, Minnesota 55455, United States

Supporting Information

ABSTRACT: Mechanistic details of the ring-opening metathesis polymerization of 3-substituted-*Z*-cyclooctenes (3RCOEs) catalyzed by the second-generation Grubbs' catalyst were systematically studied at the M06-2X/SDD|6-311+G(2df,p)//M06-L/SDD|6-31G(d) level of theory to elucidate factors contributing to observed regioselectivities. All possible conformational isomers for *Z*-cyclooctene (4 total) and 3-methyl-*Z*-cyclooctene (16 total) were taken into account. The potential energy surfaces for both the initiation and the propagation steps were calculated including all stereochemically distinct approaches of the cycloalkene to the active catalyst. In contrast to the situation with smaller cycloalkenes, the rate-limiting step for the polymerization of *Z*-cyclooctenes was determined to be the breakdown of the metallacyclobutane intermediate. This change is attributed to increased repulsive interactions between the growing polymer chain and the mesityl groups of the N-heterocyclic carbene ligand when the effective cone angle increases upon ring-opening. Most of the observed regioselectivity for 3RCOEs derives from differential steric interactions, but solvation also plays a role.

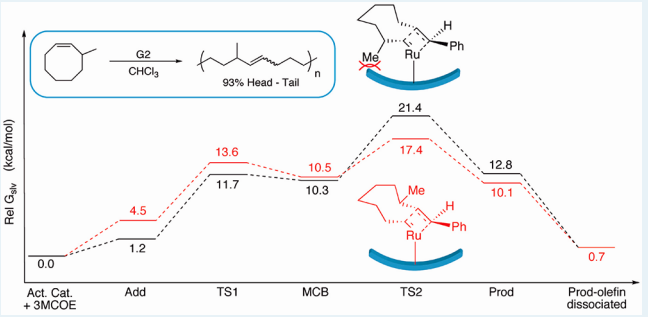

KEYWORDS: *ROMP, DFT calculations, N-heterocyclic carbene, regioselectivity, stereoselectivity, solvent effect, reaction mechanism, metathesis*

INTRODUCTION

Olefin metathesis is one of the most important and efficient methods for the generation of carbon−carbon double bonds. Acyclic diene metathesis (ADMET) polymerization and ring-opening metathesis polymerization (ROMP) are the most powerful metathesis techniques for the preparation of macromolecules. ROMP in particular generates polymers and copolymers with high molecular weights and low dispersity.[1,2] The release of ring strain energy in ROMP is the driving force to compensate for the typically positive entropy of polymerization.[3,4] ROMP is effective for many cyclic olefins possessing various functional groups.[1−34,5] This functional group tolerance allows for the preparation of a wide range of both experimentally interesting and industrially relevant polymers.

The generally accepted mechanism of ROMP (Figure 1)[1] begins with the formation of a Dewar−Chatt−Duncanson complex (alkene-metal adduct), followed by a [2+2] cycloaddition to form a metallacyclobutane intermediate (MCB). This intermediate then undergoes a retro-[2+2] that leads to the formation of a new metal alkylidene. While every step is reversible, the equilibrium is driven to the polymer product by the overall thermodynamics of the polymerization.[1,3,4] In addition to temperature and concentration, solvent choice,[6] and monomer substitution (i.e., position and functionality)[5,7] have been shown to significantly impact product molar mass and polymerization rate.

ROMP has been used extensively to generate functionalized perfectly linear polyolefins.[1,2] *Z*-cyclooctene is an ideal monomer scaffold for this approach because it has moderate ring strain (7.4 kcal/mol by one convention)[4] and is easily functionalized. Various linear low-density polyethylenes (LLDPEs) have been prepared by ROMP of 5-substituted *Z*-cyclooctenes.[5,7] However, the asymmetric nature of the substituted *Z*-cyclooctenes introduces a question of regiochemistry; head-to-head (H−H), tail-to-tail (T-T), and head-to-tail (H-T) connections have all been observed.[5] Such lack of regioselection is undesirable as polyolefin properties are highly dependent on stereo- and regiochemistry. Regioregular alkyl-branched polyethylenes have higher melting temperatures and heats of fusion than their regioirregular counterparts because of higher degrees of crystallinity.[8,9] There is thus substantial motivation to increase control of stereo- and regiochemistry in polymers derived from ROMP.

Efforts along these lines have included the exploration of variations in catalyst metal centers and ligand structures. For example, Schrock and Hoveyda have reported molybdenum catalysts where variations in ligand size yielded polymers that were highly stereoregular (cis) and in some cases syndiotac-

Received: August 13, 2012
Revised: September 10, 2012
Published: October 18, 2012

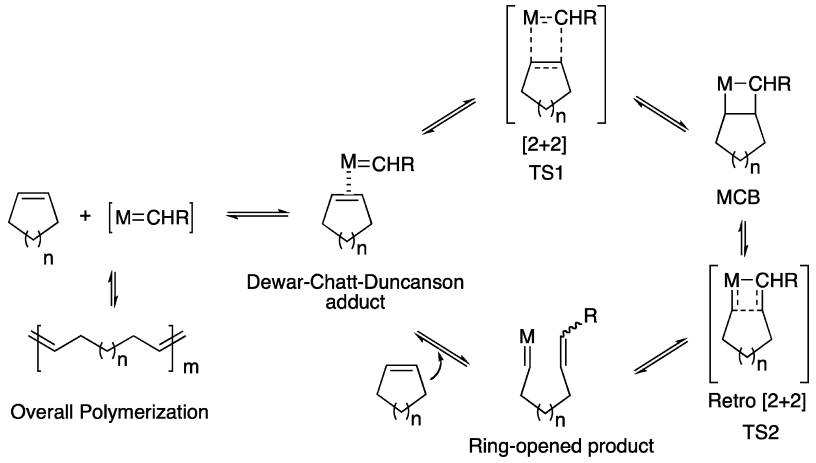

Figure 1. General mechanism of ring-opening metathesis polymerization (ROMP).

tic.[10−14] Grubbs has also designed cis-selective catalysts, where bidentate ligands play an important role.[15−19]

Besides catalyst engineering, modifying the monomer unit can also affect stereo- and regioselection. Sampson and co-workers have shown that selected 1-substituted cyclobutenes undergo ROMP to give exclusively cis H-T polymers. The stereo- and regioselectivities were attributed mainly to charge distribution at the double bond of the monomer.[20] Similarly, Wu and Grubbs reported the ROMP of 3,3-dimethylcyclobutene to give polymers with high stereoselectivity (>99% trans) and regioselectivity (>98% H-T). The authors attributed this to steric interactions between the monomer substituents and the catalyst.[21] Enantiomerically pure 3-substituted-methylcyclopentene polymerized by a Mo-based catalyst was exclusively H-T with a 3:1 trans:cis ratio.[22] Kobayashi et al. recently reported the polymerization of 3-substituted-*Z*-cyclooctenes (3RCOEs) using Grubbs' second or third generation catalysts (G2 and G3, respectively) to give polymers with high regio- (93.5−99.9% H-T) and stereoregularity (96.8−98.4% *E*).[23] The degree of regioregularity was found to increase with increasing substituent size, that is, the ratios of H-T for methyl, ethyl, hexyl and phenyl substituents were 93.5, 96.8, 98.0, and 99.9%, respectively. Although a trend between the substituent size and the stereoregularity was not observed, the *E* preference for all 3-substituted *Z*-cyclooctenes was significantly higher than that observed for unsubstituted *Z*-cyclooctene (73.4%).[23] Tungsten-based ROMP of 3-alkyl-COEs have been reported to lead to polymers that are stereoirregular and whose regioregularity has not been studied.[24,25]

Metathesis reactions involving G1 and G2 have been the subject of exhaustive experimental and computational studies.[20,26−38] Early computational analyses provided mechanistic insights but lacked quantitative accuracy in some instances because of the poor ability of early density functionals (e.g., B3LYP, BP86, and PW91) to account for attractive nonbonded interactions (dispersion) between neighboring fragments in large structures. More recent functionals (e.g., M06-L)[36−38] include such medium range attractive interactions accurately, and systematic studies have demonstrated their energetic importance for, for example, phosphine dissociation and Dewar−Chatt−Duncanson adduct formation (Figure 1).[37,38] Using the M06-L functional Truhlar and Zhao found that the Ru-phosphine bond dissociation energies (BDEs) in the gas phase are, depending on the basis set, 34.2−41.7 and 38.2−45.2 kcal/mol for G1 and G2, respectively.[37] These results are in good agreement with experimental values reported by Chen using collision induced dissociation (CID) mass spectrometry.[35]

On the basis of NMR-kinetics measurements, Grubbs and co-workers reported free energies of activation ($\Delta G^{\ddagger}$) for dissociation of the phosphine ligand from G1 and G2 catalysts in toluene to be 19.88 ± 0.06 and 23.0 ± 0.4 kcal/mol, respectively.[39,40] Using the M06-L functional and a Poisson−Boltzmann continuum solvation model, Goddard et al. calculated $\Delta G^{\ddagger}$ = 23.4 kcal/mol for phosphine dissociation from G2 in toluene,[26] which is in quantitative agreement with experiment. For the same dissociation, Jensen and co-workers calculated similar $\Delta G^{\ddagger}$ values for G1 ($\Delta G^{\ddagger}$ = 22.2 kcal/mol) and G2 ($\Delta G^{\ddagger}$ = 23.7 kcal/mol);[32] these authors also reported that the reaction free energy for phosphine dissociation (ΔG_{rxn} = 8.7 kcal/mol for G1 and ΔG_{rxn} = 9.6 kcal/mol for G2) is not equal to $\Delta G^{\ddagger}$ as other studies had assumed[29,35] (as the separated fragments can relax and are also solvated). Consequently, $\Delta G^{\ddagger}$ for the reverse phosphine−Ru association is 11.2 and 13.4 kcal/mol for G1 and G2, respectively.[32] Notwithstanding its larger phosphine dissociation activation energy, G2 is more reactive toward metathesis than G1. Truhlar et al. have demonstrated that the inverse relation between phosphine dissociation and catalyst activity is associated with the rotameric behavior of the alkylidene and the energetics associated with adopting a reactive configuration.[34]

In good agreement with experiment, computational studies on the ROMP reaction path for substituted variants of cyclobutene,[20] cyclopentene,[33] and norbornene,[26] have predicted formation of the Dewar−Chatt−Duncanson adduct to have a gas-phase enthalpy of association of about −18.0 kcal/mol (relative to infinitely separated reactants). In all of these instances, subsequent to phosphine dissociation (which generates the active catalyst) the rate-limiting step (RLS) was predicted to be the formation of the MCB intermediate for both G1 and G2. In each instance, the MCB intermediate was found to be reasonably stable on the potential energy surface (PES). Similarly, Hillier et al. studied PESs for catalyzed ring-closing metathesis (RCM) reactions leading to 5−10 member rings.[41] Considering the reverse paths on these potential energy surfaces, one again finds the RLS for ROMP to be formation of the MCB intermediate. Interestingly, though, the energy of both the MCB and the retro [2+2] transition-state (TS) structures increase relative to separated reactants with increasing ring size. Note that by considering the reverse of

dx.doi.org/10.1021/cs300549u | *ACS Catal.* 2012, 2, 2547−2556

RCM, the active catalyst incorporates a methylidine, in contrast to a larger alkylidine as one would typically find in the initiation and the propagation steps of ROMP (i.e., the initiators are typically substituted alkyidenes and the propagating species are polymeric).

In the present work, we focus on the origin of stereoselection in the ROMP of 3RCOEs with G2.[23] In particular, we exhaustively characterize stationary points on the potential energy surface for ROM of both *Z*-cyclooctene (COE) and 3-methyl-*Z*-cyclooctene (3MCOE) by G2. We consider both initiation and propagation steps and their associated Dewar−Chatt−Duncanson complexes, [2+2] TS structures, MCB intermediates, retro-[2+2] TS structures, and products.

COMPUTATIONAL METHODS

Molecular Mechanics. Exhaustive stochastic searches were employed to identify all low-energy conformations predicted for *Z*-cyclooctene and 3-methyl-*Z*-cyclooctene using the MM3 force field.[42] The resulting structures were used as starting geometries for subsequent density functional calculations. Given the excellent accuracy of MM3 for hydrocarbon conformational analysis, the relative force field energies were also used to validate the DFT model. MM3 calculations and stochastic searches made use of PC Model version 9.20.[43]

Density Functional Theory. All stationary points were fully optimized at the M06-L level of density functional theory (DFT)[44] employing the 6-31G(d) basis set[45] on all nonmetal atoms and the (8s7p6d2f)/[6s5p3d2f] basis set and associated core potential of Andrae et al. for Ru.[46] An automatically generated density-fitting basis set was employed to speed the computation of Coulomb integrals. Analytic frequency calculations were done for all structures to characterize their nature as either minima or TS structures, and also to compute thermal contributions to enthalpy and free energy employing the usual ideal-gas, rigid-rotator, quasi-harmonic-oscillator approximation to compute necessary molar partition functions.[47,48] Electronic energies were also computed for optimized structures using the M06-2X density functional,[38] which has been extensively benchmarked and shown to achieve high accuracies for organic systems; the basis set on nonmetal atoms for these single-point calculations was 6-311+G(2df,p).[45] Composite gas-phase free energies were computed as the sum of M06-2X single-point electronic energies with M06-L thermal contributions computed as described above.

Solvation. M06-2X calculations identical to those described above were also performed including the effects of chloroform solvation as computed from the SMD continuum solvation model.[49] Composite free energies in solution were computed by summing gas-phase M06-L thermal contributions with single point SMD/M06-2X single-point energies. Since the Gibbs free energies in the gas phase are calculated at 0.0446 M (1 atm), and in chloroform are reported for a standard state of 1 M, a 1.9 kcal/mol correction (equal to RT ln ([soln]/[gas])) is made to the free energy of each solute.

Software. MM3 calculations and stochastic searches made use of PC Model version 9.20.[43] All density functional calculations were accomplished with Gaussian 09 revision A.02.[50]

RESULTS

Hydrocarbon Conformational Analysis. Prior to calculating the potential energy surfaces for the ROMP of *Z*-cyclooctenes, full conformational analyses of COE and 3MCOE were done with the reliable MM3 force field.[42,51,52] We found 4 conformers for COE having relative energies of 0.0, 1.6, 3.5, and 7.0 kcal/mol, respectively. Importantly, the corresponding 298 K enthalpies from our best composite M06-2X level of DFT are 0.0 2.1, 3.8, and 6.5, validating the anticipated utility of this model for predicting conformational energy contributions to subsequent catalyzed reaction path modeling (note that MM3 was parametrized using experimental heats of formation, so a relative enthalpy is the most relevant thermodynamic quantity from DFT against which to compare). Our structures and relative energetics agree well with previously published studies of COE.[41,53,54]

To identify 3MCOE conformers expected to dominate in experimental equilibria, we considered systematic substitution of the low energy isomers of COE. As shown in Figure 2, if we limit ourselves to the two lowest ring forms of COE, each ring has 4 distinct allylic positions that my be substituted by a methyl group (labeled a, b, c, and d for the lower left structure). As the COE conformers are chiral, each of the 3MCOE structures (8 in total) that can be generated from the low-energy COE conformers has an enantiomeric form. If one considers reaction with a metal alkylidene, the asymmetry in the M=C bond leads to structures that are diastereomeric rather than enantiomeric, so we distinguish 16 conformers plausibly relevant for ROMP in Figure 2. The relative conformational energies for these species are listed in Table 1, which illustrates the enantiomeric redundancy in the absence of catalyst (e.g., the relative energy of **IIIb** is equal to that of

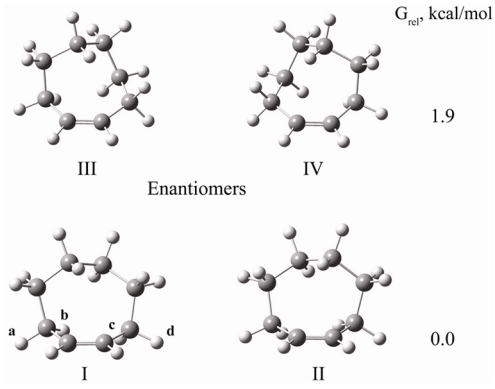

Figure 2. Low-energy conformers of COE and 3MCOE. Conformers are identified by ring form (**I**−**IV**) and substitution position (**a**−**d**). While shown only for I, allylic positions are assigned from a to d in a counterclockwise fashion starting from upper left when viewing a hypothetically flattened ring from the unsubstituted side of the double bond.

Table 1. Relative Energies (MM3) and 298 K Free Energies (M06-2X) in kcal/mol for COE and 3MCOE Conformers in Figure 2

	I		II		III		IV	
	MM3	DFT	MM3	DFT	MM3	DFT	MM3	DFT
COE	0.0	0.0	0.0	0.0	1.6	2.1	1.6	2.1
MCOE-**a**	0.0	0.0	0.5	0.2	2.8	1.9	3.7	3.4
MCOE-**b**	6.0	6.9	3.8	4.5	8.1	6.0	2.9	2.6
MCOE-**c**	3.8	4.5	6.0	6.9	2.9	2.6	8.1	6.0
MCOE-**d**	0.5	0.2	0.0	0.0	3.7	3.4	2.8	1.9

dx.doi.org/10.1021/cs300549u | *ACS Catal.* 2012, 2, 2547−2556

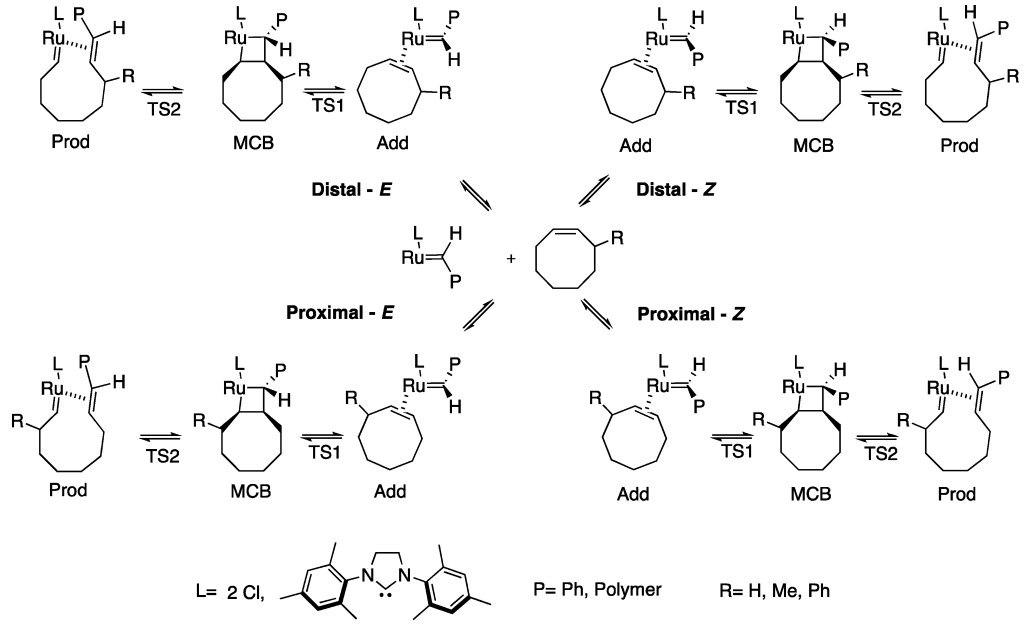

Figure 3. Possible pathways for the ROMP of 3RCOE.

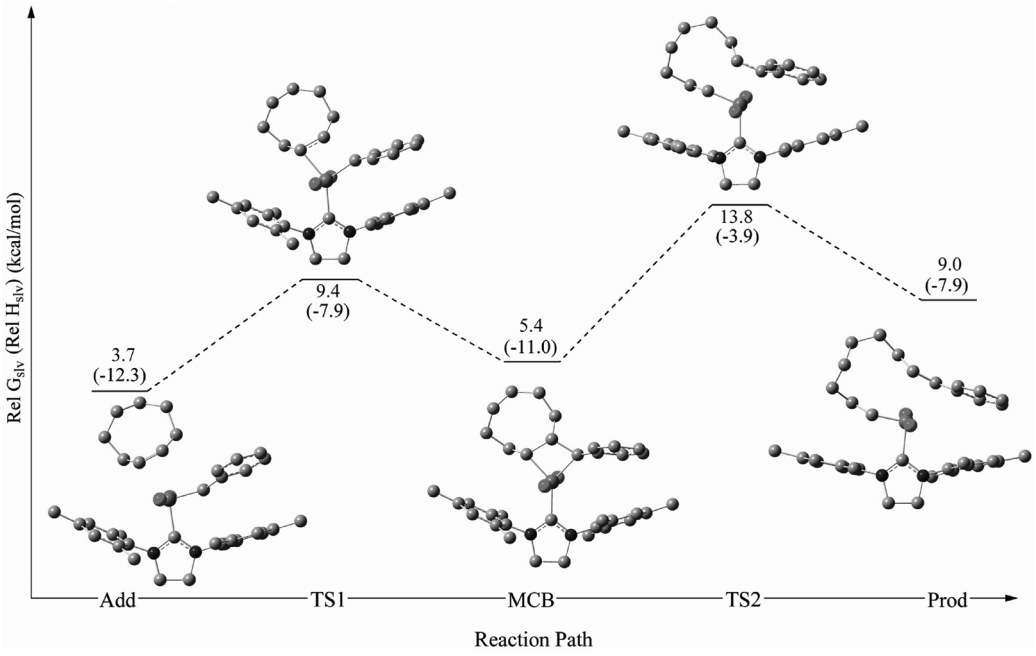

Figure 4. 298 K free energies in kcal/mol (enthalpies are in parentheses) including chloroform solvation effects for stationary points along the reaction path for **I-*E***. Hydrogen atoms are omitted for clarity.

IVc). Note that the M06-2X data in Table 1 are 298 K free energies as this will be the most convenient thermodynamic quantity with which to work moving forward, but the 298 K relative enthalpies vary by no more than 0.2 kcal/mol compared to the 298 K relative free energies. These 16 different conformers will be considered for the rest of this study. Note, though, that transannular strain makes some conformers particularly unfavorable, for example, **Ib**, **Ic**, **IIIb**, and their enantiomers.

Reaction Paths. ROMP of COE (or any cycloalkene) can produce both *Z* and *E* stereoisomers under general metathesis polymerization conditions. The inclusion of allylic functionality introduces an additional stereodistinction between the substituent being distal to the metal center or proximal to it. As a result, four possible reaction pathways can be considered (Figure 3). We proceed to characterize the potential energy surface for each pathway in Figure 3 for all conformers of COE and 3MCOE listed in Table 1.

We adopt the following nomenclature scheme for stationary points along the reaction path: Dewar−Chatt−Duncanson adduct (**Add**), [2+2] TS structure (**TS1**), metallacyclobutane intermediate (**MCB**), retro-[2+2] TS structure (**TS2**), and product (**Prod**). Unless otherwise noted, the product is itself a Dewar−Chatt−Duncanson adduct of the newly created double bond to the Ru center. We further take for our convention that the *proximal* orientations will be defined by the **a** and **b**

dx.doi.org/10.1021/cs300549u | *ACS Catal.* 2012, 2, 2547−2556

Table 2. Relative 298 K Free Energies (kcal/mol) in $CHCl_3$ for Stationary Points on the *Z* and *E* Initiation Reaction Pathways for All Four COE Conformers

	E					*Z*				
COE	Add	TS1	MCB	TS2	Prod	Add	TS1	MCB	TS2	Prod
I	3.7	9.4	5.4	**13.8**	9.0	4.7	10.4	8.3	**13.6**	6.2
II	2.7	7.8	10.2	17.2	8.7	3.2	10.8	8.3	14.3	4.2
III	5.1	15.7	12.7	21.8	6.4	6.3	14.5	11.9	19.7	9.3
IV	6.0	12.2	10.7	17.6	7.9	4.7	15.6	15.1	18.4	6.3

positions of methyl substitution in 3MCOE, while the **c** and **d** positions will define *distal*. Finally, pathways leading to cis and trans MCBs are named as ***Z*** and ***E***, respectively. As an example, **MCB-Ia-*E*** refers to the metallacyclobutane intermediate formed from reaction with conformer **I** of 3MCOE, with the methyl group in position **a** and thus *proximal* to the Ru center and an orientation leading to an ***E*** double bond in the ultimate product.

The free energy of activation for phosphine dissociation is not relevant to stereoselection and has moreover been previously calculated with excellent accuracy in both the gas phase[37] and toluene.[26,32] Thus, we began our study with the phosphine free G2 catalyst (active catalyst, Supporting Information, Figure S1). All 298 K free energies discussed below will be relative to that for the infinitely separated active catalyst and most stable COE (**I**) or 3MCOE (**Ia**) conformer. Relative enthalpy data may also be found in the Supporting Information.

Beginning with initiation, we take the active catalyst to have a phenyl carbene. Stationary points for the initiation reaction path of **I-*E*** are illustrated in Figure 4, and the relevant 298 K free energies in chloroform for all reaction paths are provided in Table 2. Note that all paths are in equilibrium with one another, so while there are four distinct paths considered for each product, there are only two non-interconverting products, namely, the *E* and *Z* styrenes. [As a technical aside, we note that substitution of the M06-L functional for the M06-2X functional in the large-basis-set single-point electronic energies increases the composite free energies of all species relative to the separated reactants by 1.5 to 2.4 kcal/mol (Supporting Information, Figure S3), but otherwise has no influence on the qualitative nature of the reactive potential energy surface. This overall insensitivity to Hartree−Fock exchange in the functional is consistent with a single dominant Kohn−Sham determinant for all species and further increases confidence in the quantitative accuracy of the M06-2X functional.]

The RLS for ROMP initiation with COE is predicted to be the retro-[2+2] of the MCB intermediate (i.e., **TS2**). This is in contrast to ROMP studies with other substrates where MCB formation via **TS1** has been predicted to be rate-determining.[20,26,33] The *E* and *Z* paths associated with conformer I of COE both have the lowest RLSs within their respective populations, indicated in boldface in Table 2 as 13.8 and 13.6 kcal/mol, respectively.

As anticipated, release of ring strain renders product formation exothermic, for example, −7.9 and −11.9 kcal/mol for **I-*E*** and **I-*Z***, respectively (see Figure 4 for enthalpy data for **I-*E***). However, the product free energies in Table 2 are positive, which initially appears inconsistent with a spontaneous polymerization reaction that proceeds with conversions over 99% under typical experimental conditions. However, the *initiation* step need not be exergonic, only the *propagation* step must be, for high conversion. More importantly, the "product" free energies in Table 2 refer to specific conformations that still include strain due to coordination of the product olefin. A related computational study of the cross metathesis of propene by Cavallo suggested that the RLS in that case is the dissociation of the product olefin.[30] In our case, if we consider the free energy change associated with dissociation of the newly formed olefin bond, we find that the activation free energy does *not* exceed that for **TS2** and that the overall free energy drops to −1.6 kcal/mol, a value which likely errs on the side of instability given the greater conformational entropy of the unfolded state that we do not attempt to assess. Furthermore, since that computation uses a single extended conformation of the growing polymer chain, it ignores the substantial entropy associated with rotation about the single bonds in the growing chain. If we make a rough assumption of $-RT$ ln 3 (roughly −0.6 kcal/mol) for the free energy associated with rotational freedom about a typical sp^3-sp^3 C−C single bond, we see that initiation *is* exergonic, albeit only modestly so.

The free energies for **TS2** in Table 2 may be used to predict a Boltzmann-weighted product distribution as shown in Table 3. The *E*:*Z* ratio is predicted to be 37:63. Such a ratio differs from the high *E* selectivity observed in COE ROMP product polymer, but we note again that the initiation step may have different stereochemical outcomes than propagation. Interestingly, in the absence of chloroform solvation, the predicted *E*:*Z* ratio is 12:88. Solvation effects will be discussed in more detail further below.

Table 3. 298 K Boltzmann-Weighted Product Populations for COE Initiation in $CHCl_3$

COE	G_{rel} **TS2** (kcal/mol)	population	total
I-*E*	0.2	0.37	37%
II-*E*	3.6	0.00	
III-*E*	8.2	0.00	
IV-*E*	4.0	0.00	
I-*Z*	0.0	0.47	63%
II-*Z*	0.7	0.16	
III-*Z*	6.1	0.00	
IV-*Z*	4.8	0.00	

Turning next to 3MCOE, Table 4 provides free energy results for the two lowest-energy initiation step pathways, which corresponded to methyl substitution at the **a** or **d** positions. As noted above, methyl groups in the **b** or **c** positions lead to higher energies owing to increased transannular interactions. The free energies of **b** and **c** pathways and the enthalpies for *all* pathways are provided in Supporting Information.

As found for COE, TS2 is also predicted to correspond to the RLS for the formation of 3MCOE product. The lowest activation free energy corresponding to each non-interconvert-

dx.doi.org/10.1021/cs300549u | *ACS Catal.* 2012, 2, 2547−2556

Table 4. Relative 298 K Free Energies (kcal/mol) in $CHCl_3$ for Stationary Points on Initiation Reaction Pathways for Selected 3MCOE Conformers

	E					*Z*				
MCOE	Add	TS1	MCB	TS2	Prod	Add	TS1	MCB	TS2	Prod
Ia	1.2	11.7	10.3	**21.4**	12.8	2.1	13.2	12.0	**18.7**	8.5
IIa	1.1	9.9	10.2	25.8	14.2	1.8	12.3	11.3	19.7	9.2
IIIa	5.1	16.4	15.7	29.1	12.7	4.2	16.3	14.3	23.0	10.8
IVa	6.3	13.2	13.4	25.2	10.5	6.3	15.7	15.5	21.1	9.9
Id	4.5	13.6	10.5	**17.4**	10.1	5.2	21.7	20.5	24.4	7.1
IId	3.3	13.1	8.5	17.9	9.6	5.2	19.8	16.3	22.3	6.6
IIId	6.2	17.1	16.5	19.3	12.7	6.7	17.1	15.8	**20.2**	8.1
IVd	5.7	17.1	15.1	17.9	10.7	5.6	22.8	21.6	22.4	8.0

ing product is indicated in boldface in Table 4, and the lowest of all is 17.4 kcal/mol for **Id-*E***, which is consistent with the methyl substituent reacting in the *distal* orientation as has been found experimentally when 1 equiv of 3MCOE was reacted with 1 equiv of G2.[23] Also as found for COE, dissociation of the newly formed double bond leads to a substantially reduced product free energy of, for example, 0.7 kcal/mol for *E*; accounting for growing chain entropy would likely predict this reaction to be weakly exergonic. Boltzmann-weighted product distributions derived from the data in Table 4 are provided in Table 5. Chloroform solvation is again predicted to play a role as it increases the product population of *distal* isomer to 93% from a gas-phase value of 49% (see Supporting Information, Table S3). In the case of MCOE, the preference for the *E* isomer is clear and consistent with experimental results.

Table 5. 298 K Boltzmann-Weighted Product Populations for 3MCOE Initiation in $CHCl_3$

COE	G_{rel} TS2 (kcal/mol)	population	total
Ia-E	4.0	0	0%
IIa-E	8.4	0	
IIIa-E	11.7	0	
IVa-E	7.8	0	
Ia-Z	1.3	0.06	7%
IIa-Z	2.3	0.01	
IIIa-Z	5.6	0	
IVa-Z	3.7	0	
Id-E	0.0	0.51	93%
IId-E	0.6	0.2	
IIId-E	1.9	0.02	
IVd-E	0.6	0.2	
Id-Z	7.0	0	0%
IId-Z	4.9	0	
IIId-Z	2.8	0	
IVd-Z	5.0	0	

Noting the degree to which only a few low energy paths contributed to the initiation reactivity of 3MCOE, we reduced our focus to these paths and considered propagation next. To model propagation, we replaced the benzylidene group in the active catalyst with a propylidene group deemed to be a more realistic mimic of the growing polymer chain **P**. Relevant stationary-point 298 K free energies and Boltzmann-weighted product distributions are presented in Table 6.

The RLS for propagation continues to be predicted to be **TS2**, but the free energies of activation are considerably lower than those predicted for the initiation step (cf. Table 4). While the Boltzmann predictions suggest a lower regioselectivity for the propagation step, the *distal* orientation is still preferred. A solvent effect is again observed to contribute to the preference for distal product, but the magnitude is small.

DISCUSSION

ROM of COE. Our predicted enthalpies for complexation of *Z*-cyclooctene to activated G2 (Supporting Information, Table S4) are in good agreement with those previously reported for other cycloalkenes using quantum mechanical models that accurately include dispersion effects.[34,35] Figure 4 representatively illustrates COE approach to the ruthenium center trans to the NHC ligand with the benzylidene rotated to a reactive conformation. Formation of the **MCB** proceeds through a [2+2] cycloaddition (**TS1**) that is concerted and asynchronous. The retro-[2+2] breakdown (**TS2**) of **MCB** is also concerted and asynchronous and generates a new double bond coordinated to the Ru center.

Previous computational results on substituted cyclobutenes,[20] cyclopentenes,[33] and norbornene[26] have predicted that, subsequent to phosphine dissociation, the RLS is the

Table 6. Relative 298 K Free Energies (kcal/mol) in $CHCl_3$ for Stationary Points on Propagation Reaction Pathways for Selected 3MCOE Conformers and Associated Boltzmann-Weighted Product Populations

	Add	TS1	MCB	TS2	Prod	G_{rel} TS2 (kcal/mol)	population	total
Ia-*E*-P	0.3	7.1	6.6	17.8	8.2	4.3	0.00	33%
Ia-*Z*-P	1.2	6.9	7.8	13.7	10.5	0.2	0.31	
IIa-*E*-P	0.1	6.5	6.6	22.2	9.2	8.7	0.00	
IIa-*Z*-P	1.9	6.9	6.1	15.3	12.7	1.8	0.02	
Id-*E*-P	1.0	12.0	8.4	**13.5**	5.4	0.0	0.44	67%
IId-*E*-P	2.2	10.5	5.7	14.3	6.1	0.8	0.11	
IVd-*E*-P	2.9	14.0	11.1	14.3	6.1	0.8	0.11	

dx.doi.org/10.1021/cs300549u | *ACS Catal.* 2012, 2, 2547−2556

formation of the MCB intermediate via **TS1**, which contrasts with our predictions for COE (Table 2). To examine this disparity more closely, analogous stationary points for the ROMP of norbornene, cyclopentene, and cycloheptene were calculated in the gas phase at the composite M06-2X level and compared to our COE results (Figure 5).

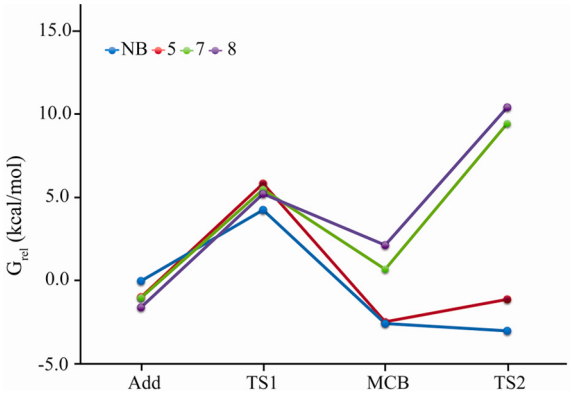

Figure 5. Gas-phase 298 K free energies for stationary points associated with the *E*-ROMP of Norbornene (NB), *Z*-cyclopentene (5), *Z*-cycloheptene (7), and *Z*-cyclooctene (8).

The data in Figure 5 suggest that as the ring size increases, the stability of the MCB intermediate relative to the initial adduct decreases. This presumably derives from increased steric interactions when the larger hydrocarbon is brought into closer contact with other catalyst functionality upon MCB formation. In addition, cyclopentane, cycloheptane, and cyclooctane have higher ring strain energies (0.39, 0.87, and 4.3 kcal/mol, respectively) than their corresponding cycloalkenes,[55] and this also comes into play upon MCB formation. A similar trend was observed by Hillier et al. in the ring closing metathesis (RCM) of a series of α,ω dienes to form 5 to 10 member rings.[41]

Figure 5 also shows that as the ring size increases the RLS changes. For norbornene and cyclopentene it is **TS1** but for cycloheptene and cyclooctene it is **TS2**. The change is entirely attributable to differences in the nature of **TS2** across the different rings, as in all cases the relative free energy of **TS1** is predicted to be about the same (Table 7).

Table 7. Relative Gas-Phase 298 K Free Energies (kcal/mol) for Stationary Points Associated with the *E*-ROMP of Norbornene (NB), *Z*-cyclopentene (5), *Z*-cycloheptene (7), and *Z*-cyclooctene (8)

ring size	Add	TS1	MCB	TS2
NB	0.0	4.2	−2.6	−3.0
5	−1.0	5.8	−2.5	−1.1
7	−1.0	5.5	0.7	9.4
8	−1.6	5.2	2.1	10.4

The influence of ring size on the relative energy of **TS2** may be best understood through consideration of the cone angle θ defined by the positions of the two "lowest" atoms associated with the polymer chain fragment on either side of the ruthenium center (see Figure 6). Table 8 provides cone angles for different reacting ring sizes. Large cone angles are associated with increased repulsive interactions between the opening ring and either or both mesityl groups of the N-heterocyclic carbene (NHC). This observation rationalizes the larger **TS2** free

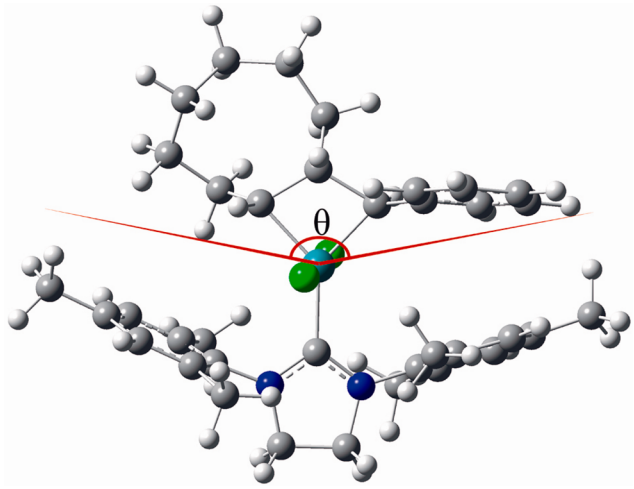

Figure 6. Defining the cone angle θ for **I-MCB-*E***.

Table 8. M06-L Cone Angles (deg) for Stationary Points of Different Ring Sizes on *E* Reaction Paths

ring size	Add	TS1	MCB	TS2
NB[a]	157	121	136	144
5[a]	143	139	140	150
7[a]	134	139	145	164
8[a]	136	146	146	167
H-5[b]	138	126	120	120
H-7[b]	141	133	130	140
H-8[b]	150	139	135	142

[a]Calculations performed in this work. [b]Data from RCM stationary points reported by Hillier et al.[41]

energies of activation for larger rings, and also the larger value computed for initiation than for propagation, since the phenyl ring increases the cone angle (illustrated in Figure 6) relative to an alkyl chain. We note also that in RCM the effect persists but is minimized as the methylidene component keeps one "side" of the cone reduced in size (cf. data from Hillier et al.[41] in Table 8).

ROM of 3MCOE. Figure 7 shows a representative *E* free energy diagram for distal (**Id-*E***) and proximal (**Ia-*E***) substrate approaches for the initiation step. The *proximal* approach has the lower free energy of activation for the formation of **MCB**, but the **MCB** intermediates themselves have nearly identical free energies. The RLS (**TS2**) is considerably lower in free energy for the path leading to *distal* product (See Figure 8). As noted previously for COE, the free energy change is rendered much more favorable by dissociation of the newly formed double bond.

When the free energies for 3MCOE stationary points (Table 4) are compared to their unsubstituted COE analogs (Table 2), it is evident that the former are higher, including for the RLS. A reduction in polymerization rate would be predicted on this basis and that agrees with what is known experimentally.[23] As noted above, the results in Tables 4 and 5 predict distal regioselectivity for the initiation step, which agrees with experiment. That is, the methyl substituent in the **d** position, *distal* to the Ru center, is preferred over the substituent in the **a** position. This can again be attributed to steric interactions in **TS2**. Compared to COE or **d**-3MCOE, the presence of the methyl substituent in position **a** increases the cone angle significantly along the reaction pathway (Figure 8), which

dx.doi.org/10.1021/cs300549u | *ACS Catal.* 2012, 2, 2547−2556

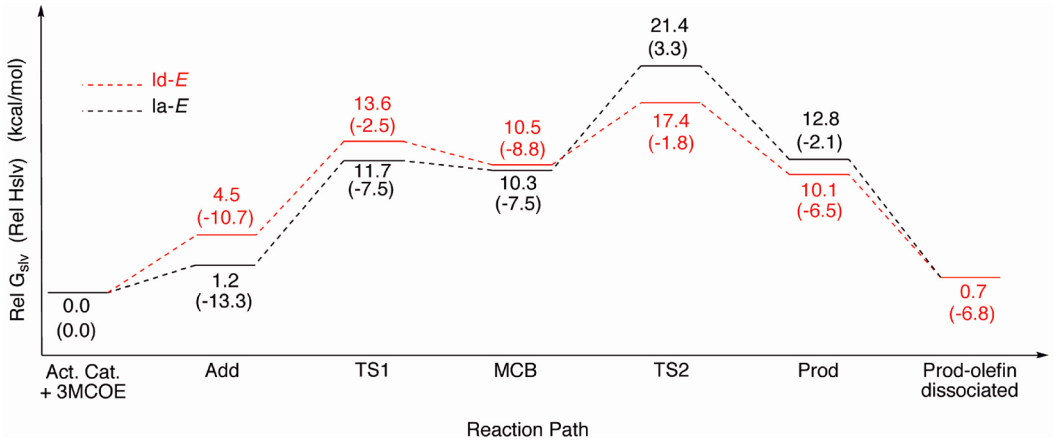

Figure 7. 298 K free energies and enthalpies (kcal/mol, enthalpies in parentheses) including chloroform solvation effects for stationary points along the two lowest energy trans reaction paths (**Id-*E*** and **Ia-*E***) for the ROMP initiation of 3MCOE in $CHCl_3$.

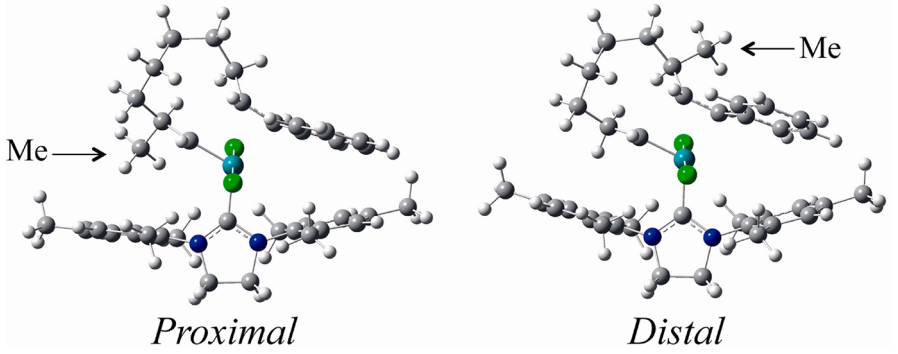

Figure 8. Optimized M06-L *E* **TS2** structures for the *proximal* and *distal* reactions of 3MCOE.

increases repulsive interactions with the mesityl groups of the NHC ligand. Indeed, a comparison of cone angle data (Supporting Information, Table S17) with energetic data in Tables 2 and 4 shows a direct relationship between larger cone angles and increased relative free energies in all instances.

Interestingly, for initiation the **TS2** cone angles for the *Z* pathways are smaller than those for the *E* pathways in all cases. This is particularly important for the proximal approach as it lowers the free energy of activation of the RLS considerably, although the proximal approach remains disfavored compared to distal.

Although the dominant influence on regioselectivity is steric in origin, the preference for distal vs proximal approach increases when solvent effects are included. In the gas phase the two possible approaches for the initiation step are computed to lead to a nearly 1:1 (distal: proximal) product distribution. When $CHCl_3$ solvation is taken into account the ratio increases to 93:7 (distal:proximal), which matches experiment well.[23] This effect is attributable to the greater polarity of distal TS2 structures compared to proximal ones. This polarity is manifest in computed dipole moments (Table 9). Interestingly, in all cases dipole moments are also higher for *E* **TS2** structures than for *Z*, which rationalizes solvent influence on that stereochemistry as well.

Propagation. As noted above, relative free energies predicted for propagation paths are considerably lower than those for initiation. This is attributable to the reduced steric demands of the propylidene group compared to the benzylidene in the various stationary point structures. In the gas phase, the distal approach is preferred for the initiation step,

Table 9. M06-2X Dipole Moments (*D*) for TS Structures on Selected Initiation Step Pathways

	E		*Z*	
COE	**TS1**	**TS2**	**TS1**	**TS2**
I	2.63	3.01	3.03	2.72
II	2.58	2.93	2.89	2.80
III	2.81	2.99	3.10	2.52
IV	2.77	3.13	3.17	2.94
Ia	2.99	3.14	3.10	2.67
IIa	2.95	2.66	3.20	2.64
IIIa	3.15	2.74	3.19	2.52
IVa	2.91	2.68	3.21	3.28
Id	2.52	3.17	3.18	3.04
IId	2.51	2.95	3.27	3.14
IIId	2.87	3.29	3.23	3.13
IVd	2.62	3.27	3.09	3.01

and, as found for initiation, upon inclusion of solvent effects this preference is increased.

To assess the influence of the allylic substituent on the ROMP regioselectivity, we examined propagation step paths for 3-phenyl-*Z*-cyclooctene (3PCOE), and in particular the analogues to **Ia-*E***, **Ia-*Z***, **Id-*E***, and **IId-*E***. 3PCOE was observed to give the highest regioselectivity experimentally (99.9%).[23] The bulkier substituent is indeed predicted to increase steric bias in competing TS structures, and we predict 100% selectivity for the distal approach in both the gas phase and

dx.doi.org/10.1021/cs300549u | *ACS Catal.* 2012, 2, 2547−2556

solution (Supporting Information, Table S16). The repulsive interactions of the phenyl substituent with a mesityl group in the proximal approach are so significant that the NHC group is noticeably distorted in the corresponding **TS2** (Supporting Information, Figure S2). Interestingly, the free energy of activation for the distal **TS2** of 3PCOE is lower than that for 3MCOE. This likely reflects stabilizing conjugation effects associated with the forming styrene moiety developing in the TS structure.

CONCLUSIONS

ROMP of *Z*-cyclooctene by Grubbs' second generation catalyst has a different rate-limiting step than that for smaller rings such as cyclopentene. While for smaller rings the formation of a metallacyclobutane intermediate via a [2+2] cycloaddition is the rate limiting step, for larger rings it is the breakdown of that same intermediate via a retro-[2+2] step that is rate limiting. Two factors contribute to this change, increased differential ring strain between the intermediate cycloalkane and the precursor cycloalkene (in the case of COE) and increased repulsive interactions between larger cycloalkanes and the mesityl groups of the NHC ligand, particularly in the retro-[2+2] step. 3-substituted *Z*-cyclooctenes prefer reaction paths leading to distal products compared to proximal ones as significant repulsive interactions between the allylic substituent and the NHC mesityl ligands are implicit in the latter. Solvation effects modestly favor distal over proximal reactions owing to greater polarity of the relevant rate-determining transition-state structures for the former. These observations provide microscopic insight into factors that can be tuned to control stereo- and regioselectivity in the design of future ROMP substrates and catalysts.

ASSOCIATED CONTENT

Supporting Information

Free energies and enthalpies (kcal/mol) in both gas phase and chloroform for all calculated potential energy surfaces. Cartesian Coordinates for all structures optimized at the M06-L/SDDl6-31G(d) level of theory are provided as well. This material is available free of charge via the Internet at http://pubs.acs.org.

AUTHOR INFORMATION

Corresponding Author

*E-mail: hillmyer@umn.edu (M.A.H.), cramer@umn.edu (C.J.C.).

Notes

The authors declare no competing financial interest.

ACKNOWLEDGMENTS

This work was supported by the UMN Initiative for Renewable Energy and the Environment (RL-0015-11) and by the U.S. National Science Foundation (CHE-0952054). Partial support from the Dow Chemical Company is also acknowledged.

REFERENCES

(1) Bielawski, C. W.; Grubbs, R. H. *Prog. Polym. Sci.* **2007**, *32*, 1.
(2) Schrock, R. R. *Acc. Chem. Res.* **1990**, *23*, 158.
(3) Hejl, A.; Sherman, O. A.; Grubbs, R. H. *Macromolecules* **2005**, *38*, 7214.
(4) Walker, R.; Conrad, R. M.; Grubbs, R. H. *Macromolecules* **2009**, *42*, 599.
(5) Hillmyer, M. A.; Laredo, W. R.; Grubbs, R. H. *Macromolecules* **1995**, *28*, 6311.
(6) Al Samak, B.; Amir-Ebrahimi, V.; Corry, D. G.; Hamilton, J. G.; Rigby, S.; Rooney, J. J.; Thompson, J. M. *J. Mol. Catal. A: Chem* **2000**, *160*, 13.
(7) Mutch, A.; Leconte, M.; Lefebvre, F.; Basset, J.-M. *J. Mol. Catal. A: Chem.* **1998**, *133*, 191.
(8) Rojas, G.; Berda, E. B.; Wagener, K. B. *Polymer* **2008**, *49*, 2985.
(9) Rojas, G.; Wagener, K. B. *Macromolecules* **2009**, *42*, 1934.
(10) Singh, R.; Schrock, R. R. *Macromolecules* **2008**, *41*, 2990.
(11) Flook, M. M.; Gerber, L. C. H.; Debelouchina, G. T.; Schrock, R. R. *Macromolecules* **2010**, *43*, 7515.
(12) Ismail, I.; Miao, Y.; Schrock, R. R.; Hoveyda, A. H. *J. Am. Chem. Soc.* **2009**, *131*, 3844.
(13) Jiang, A. J.; Zhao, Y.; Schrock, R. R.; Hoveyda, A. H. *J. Am. Chem. Soc.* **2009**, *131*, 16630.
(14) Gerber, L. C. H.; Schrock, R. R.; Muller, P.; Takase, M. K. *J. Am. Chem. Soc.* **2011**, *133*, 18142.
(15) Endo, K.; Grubbs, R. H. *J. Am. Chem. Soc.* **2011**, *133*, 8525.
(16) Keitz, B. K.; Endo, K.; Herbert, M. B.; Grubbs, R. H. *J. Am. Chem. Soc.* **2011**, *133*, 9686.
(17) Keitz, B. K.; Endo, K.; Patel, P. R.; Herbert, M. B.; Grubbs, R. H. *J. Am. Chem. Soc.* **2012**, *134*, 693.
(18) Liu, P.; Xu, X.; Dong, X.; Keitz, B. K.; Herbert, M. B.; Grubbs, R. H.; Houk, K. N. *J. Am. Chem. Soc.* **2012**, *134*, 1464.
(19) Keitz, B. K.; Fedorov, A.; Grubbs, R. H. *J. Am. Chem. Soc.* **2012**, *134*, 2040.
(20) Song, A.; Chul-Lee, J.; Parker, K.; Sampson, N. S. *J. Am. Chem. Soc.* **2010**, *132*, 10513.
(21) Wu, Z.; Grubbs, R. H. *Macromolecules* **1995**, *28*, 3502.
(22) Sita, L. R. *Macromolecules* **1995**, *28*, 656.
(23) Kobayashi, S.; Pitet, L. M.; Hillmyer, M. A. *J. Am. Chem. Soc.* **2011**, *133*, 5794.
(24) Gianotti, G.; Dall'Asta, G.; Valvassori, A.; Zamboni, V. *Makromol. Chem* **1971**, *149*, 117.
(25) Calderon, N.; Ofstead, E. A.; Judy, W. A. *J. Polym. Sci., Part A: Polym. Chem.* **1967**, *5*, 2209.
(26) Benitez, D.; Tkatchouk, E.; Goddard, W. A., III *Organometallics* **2009**, *28*, 2643.
(27) Benitez, D.; Tkatchouk, E.; Goddard, W. A., III *Chem. Commun.* **2008**, 6194.
(28) Bernardi, F.; Bottoni, A.; Miscione, G. P. *Organometallics* **2003**, *22*, 940.
(29) Fomine, S.; Martinez, S.; Tlenkopatchev, M. A. *Organometallics* **2003**, *22*, 93.
(30) Bahri-Laleh, N.; Credendino, R.; Cavallo, L. *Beilstein J. Org. Chem.* **2011**, *7*, 40.
(31) Straub, B. F. *Adv. Synth. Catal.* **2007**, *349*, 204.
(32) Minenkov, Y.; Occhipinti, G.; Heyndrickx, W.; Jensen, V. R. *Eur. J. Inorg. Chem.* **2012**, *9*, 1507.
(33) Rowley, C. N.; Van der Eide, E. F.; Piers, W. E.; Woo, T. K. *Organometallics* **2008**, *27*, 6043.
(34) Yang, H.-C.; Huang, Y.-C.; Lan, Y.-K.; Luh, T.-Y.; Zhao, Y.; Truhlar, D. G. *Organometallics* **2012**, *30*, 4196.
(35) Torker, S.; Merki, D.; Chen, P. *J. Am. Chem. Soc.* **2008**, *130*, 4808.
(36) Zhao, Y.; Truhlar, D. G. *J. Chem. Phys.* **2006**, *124*, 224105.
(37) Zhao, Y.; Truhlar, D. G. *Org. Lett.* **2007**, *9*, 1967.
(38) Zhao, Y.; Truhlar, D. G. *Acc. Chem. Res.* **2008**, *41*, 157.
(39) Sanford, M. S.; Love, J. A.; Grubbs, R. H. *J. Am. Chem. Soc.* **2001**, *123*, 6543.
(40) Sanford, M. S.; Ulman, M.; Grubbs, R. H. *J. Am. Chem. Soc.* **2001**, *123*, 749.
(41) Hillier, I. H.; Pandian, S.; Percy, J. M.; Vincent, M. A. *Dalton Trans.* **2011**, *40*, 1061.
(42) Allinger, N. L.; Yuh, Y. H.; Lii, J. H. *J. Am. Chem. Soc.* **1989**, *111*, 8551.
(43) *PC Model*, version 9.2; Serena Software: Bloomington, IN, 2010.
(44) Zhao, Y.; Truhlar, D. G. *J. Chem. Phys.* **2006**, *125*, 194101.

(45) Hehre, W. J.; Radom, L.; Schleyer, P. v. R.; Pople, J. A. *Ab Initio Molecular Orbital Theory*; Wiley: New York, 1986.
(46) Andrae, D.; Häußermann, U.; Dolg, M. S., H.; Preuß, H. *Theor. Chem. Acc.* **1990**, *77*, 123.
(47) Cramer, C. J. *Essentials of Computational Chemistry: Theories and Models*, 2nd ed.; John Wiley & Sons: Chichester, U.K., 2004.
(48) Ribeiro, R. F.; Marenich, A. V.; Cramer, C. J.; Truhlar, D. G. *J. Phys. Chem. B* **2011**, *115*, 14556.
(49) Marenich, A. V.; Cramer, C. J.; Truhlar, D. G. *J. Phys. Chem. B* **2009**, *113*, 6378.
(50) Frisch, M. J.; Trucks, G. W.; Schlegel, H. B.; Scuseria, G. E.; Robb, M. A.; Cheeseman, J. R.; Scalmani, G.; Barone, V.; Mennucci, B.; Petersson, G. A.; Nakatsuji, H.; Caricato, M.; Li, X.; Hratchian, H. P.; Izmaylov, A. F.; Bloino, J.; Zheng, G.; Sonnenberg, J. L.; Hada, M.; Ehara, M.; Toyota, K.; Fukuda, R.; Hasegawa, J.; Ishida, M.; Nakajima, T.; Honda, Y.; Kitao, O.; Nakai, H.; Vreven, T.; Montgomery, J. A.; Peralta, J. E.; Ogliaro, F.; Bearpark, M.; Heyd, J. J.; Brothers, E.; Kudin, K. N.; Staroverov, V. N.; Kobayashi, R.; Normand, J.; Raghavachari, K.; Rendell, A.; Burant, J. C.; Iyengar, S. S.; Tomasi, J.; Cossi, M.; Rega, N.; Millam, J. M.; Klene, M.; Knox, J. E.; Cross, J. B.; Bakken, V.; Adamo, C.; Jaramillo, J.; Gomperts, R.; Stratmann, R. E.; Yazyev, O.; Austin, A. J.; Cammi, R.; Pomelli, C.; Ochterski, J. W.; Martin, R. L.; Morokuma, K.; Zakrzewski, V. G.; Voth, G. A.; Salvador, P.; Dannenberg, J. J.; Dapprich, S.; Daniels, A. D.; Farkas, Ö.; Foresman, J. B.; Ortiz, J. V.; Cioslowski, J.; Fox, D. J. *Gaussian 09*, Revision A.02; Gaussian, Inc.: Wallingford, CT, 2010.
(51) Lii, J. H.; Allinger, N. L. *J. Am. Chem. Soc.* **1989**, *111*, 8566.
(52) Lii, J. H.; Allinger, N. L. *J. Am. Chem. Soc.* **1989**, *111*, 8576.
(53) Penman, K. G.; Kitching, W.; Wells, A. P. *J. Chem. Soc., Perkin Trans. 1* **1991**, 721.
(54) Neuenschwander, U.; Hermans, I. *J. Org. Chem.* **2011**, *76*, 10236.
(55) von R. Schleyer, P.; Williams, J. E., Jr. *J. Am. Chem. Soc.* **1970**, *92*, 2377.

NOTE ADDED AFTER ASAP PUBLICATION

After this paper was published online November 1, 2012, a sentence was added to the Acknowledgments. The corrected version was reposted November 2, 2012.